Macromolecular Research, Vol. 15, No. 6, pp 513-519 (2007)

In Vitro Cellular Uptake and Cytotoxicity of Paclitaxel-Loaded Glycol Chitosan Self-Assembled Nanoparticles

Ji Sun Park

College of Medicine, Pochon Cha University, Seoul 135-081, Korea

Yong Woo Cho*

Department of Chemical Engineering, Hanyang University, Ansan 426-791, Korea

Received March 19, 2007; Revised July 20, 2007

Abstract: Self-assembled nanoparticles have great potential to act as vehicles for hydrophobic drug delivery. Understanding nanoparticle cellular internalization is essential for designing drugs intended for intracellular delivery. Here, the endocytosis and exocytosis of fluorescein isothiocyanate (FITC)-conjugated glycol chitosan (FGC) self-assembled nanoparticles were investigated by flow cytometry and confocal microscopy. The cellular internalization of FGC nanoparticles was initiated by nonspecific interactions between nanoparticles and cell membranes. Although adsorptive endocytosis of the nanoparticles occurred quickly, significant amounts of FGC nanoparticles were exocytosed, particularly in the early stage of endocytosis. The amount of exocytosed nanoparticles was dependent on the pre-incubation time with nanoparticles, suggesting that exocytosis is dependent on the progress of endocytosis. FGC nanoparticles internalized by adsorptive endocytosis were distributed in the cytoplasm, but not in the nucleus. *In vitro* cell cycle analysis demonstrated that FGC nanoparticles delivered paclitaxel into the cytoplasm and were effective in arresting cancer cell growth.

Keywords: nanoparticles, chitosan, drug delivery, endocytosis, exocytosis, paclitaxel, cytotoxicity.

Introduction

Polymer nanoparticles are colloidal vesicular systems that vary in size from 10 to 1,000 nm and have been actively studied as a potential drug delivery system.[1-3] Polymeric amphiphiles that have an appropriate hydrophilic/hydrophobic balance form self-assembled nanoparticles in aqueous milieu. The hydrophobic cores of self-assembled nanoparticles serve as a depot for accommodating predominantly hydrophobic drugs, and the shells provide colloidal stability in an aqueous milieu and can interact with cell membranes.

Chitosan, which is mainly composed of 2-amino-2-deoxy-β-D-glucopyranose (D-gluocosamine), is one of the most abundant natural polysaccharides. Indeed, chitosan is a versatile carrier for delivering drugs and genes.[4-6] This polysaccaharide has reactive amino groups at the C2 position of glucosamine, which can be readily used for chemical modification, conjugation with drugs and cell/tissue-targeting moieties, as well as for forming complexes with oligonucleotides, siRNA, and DNA. The attachment of hydrophobic moieties (doxorubicin (DOX), deoxycholic acid (DOCA), and fluorescein isothiocyanate (FITC)) to chitosan induces the amphiphilic conjugates to form nanosized supramolecular self-assemblies.[7-15] For efficient drug and gene deliveries, detailed insight into the behavior of chitosan nanoparticles during cellular processes such as endocytosis, exocytosis, and intracellular drug release is essential. To date, only limited information is available on the interaction between chitosan nanoparticles and cells.[16-19] Understanding the series of events involved in cellular internalization of nanoparticles may provide a rationale for designing tailor-made nanoparticles in order to increase intracellular drug delivery.

Here, we report on the cellular uptake of glycol chitosan (GC) nanoparticles and the cytotoxicity of paclitaxel-loaded GC nanoparticles. Fluorescein isothiocyanate (FITC)-conjugated glycol chitosan (FGC) self-assembled nanoparticles were prepared for intracellular trafficking. Flow cytometric analysis and confocal microscopy were used to monitor the internalization of FGC nanoparticles. Paclitaxel, a drug widely used in the clinical treatment of cancer, was incorporated into FGC nanoparticles, and the cytotoxicity of these nanoparticles on human cancer cell lines was investigated by cell cycle analysis.

*Corresponding Author. E-mail: ywcho7@hanyang.ac.kr

Experimental

Materials. Glycol chitosan (GC, MW 250 kDa, degree of deacetylation 88.7%) was purchased from Sigma (St. Louis, MO, USA), dissolved in distilled water, filtered to remove insoluble impurities, and dialyzed against distilled water. Fluorescein isothiocyanate (FITC), chloroform, paclitaxel (PTX), and bovine serum albumin (BSA, Fraction V) were purchased from Sigma and used without further purification. Dulbecco's modified Eagle's medium (DMEM), fetal bovine serum (FBS), RPMI-1640 medium (RPMI), trypsin-EDTA (0.5% trypsin, 5.3 mM EDTA tetra-sodium), and penicillin-streptomycin (100 U/mL) were purchased from Gibco BRL (Rockville, MD, USA). All other chemicals were of analytical grade and were used as received.

Preparation of FGC Self-Assembled Nanoparticles. FGC nanoparticles were prepared in a manner similar to the previously described procedure.[10,14,15] The FITC content in the FGC conjugate was determined using a fluorometer (GENios, Tecan, Austria) based on the standard curve obtained from FITC alone. FGC nanoparticle suspensions were sonicated for 2 min using a probe-type sonicator (Ultrasonic Processor GEX-600, Sigma) at 90 W, in which the pulse was turned off for 1 s after 5 s sonification intervals. The nanoparticle suspensions were passed through a syringe filter (pore size 0.45 μm, Millipore, Billerica, MA, USA) and stored at room temperature. The particle size and size distribution of the self-assembled nanoparticles were measured by dynamic light scattering (DLS) using a helium ion laser system (Spectra Physics Laser Model 127-35, Mountain View, CA, USA).

Paclitaxel Loading into FGC Self-Assembled Nanoparticles. FGC nanoparticles (10 mg) were suspended in PBS (1 mL) with gentle shaking for 3 h. 0.1 mg of PTX in 100 μL chloroform was slowly added to the suspension and the resulting mixture was stirred for 24 h. Next, the chloroform was evaporated and the suspension was centrifuged to remove PTX precipitates. Finally, the supernatant was collected, passed through a cellulose acetate syringe filter (pore size 0.80 μm, Millipore), and freeze-dried. The PTX content in the FGC nanoparticles was measured using HPLC.

Cell Culture. NIH3T3 (mouse fibroblast cell line), SCC7 (mouse squamous carcinoma cell line), HeLa (human epithelioid cervical cancer cell line), MDA-MB231 (human breast cancer cell line), and A549 (human lung cancer cell line) were obtained from the American Type Culture Collection (ATCC, Manassas, VA, USA). These cell lines were routinely cultured in RPMI-1640 or DMEM media containing 10% fetal bovine serum (FBS) and 1% penicillin-streptomycin at 37 °C, 5% CO_2, and 95% humidity.

Cellular Uptake of FGC Nanoparticles. Cells were plated in a 6-well culture dish and cultured at 37 °C in 5% CO_2 until 80% confluent. Cells were rinsed twice and pre-incubated for 1 h with 2 mL of serum-free medium at 37 °C. FGC nanoparticles were added at particle concentrations ranging from 0.01 to 0.2 mg/mL and incubated at 37 °C for periods ranging from 30 min to 24 h. The cells were washed three times with 1 mL of PBS (pH 7.4) to remove any free FGC nanoparticles, detached with 0.25% trypsin, and centrifuged at 1200 rpm. Supernatants were discarded and the cells were re-suspended in PBS containing 0.1% BSA. Cells were fixed in a 3.7% paraformaldehyde solution at 4 °C, washed three times with PBS, re-suspended in PBS, and introduced into a FACSCalibur flow cytometer (Becton Dickinson, San Jose, CA, USA) that was equipped with a 488-nm argon ion laser. The data presented are the mean fluorescent signals for 10,000 cells.

Confocal Microscopy. Cells were seeded into 8-well chambers (Lab-Tek^R, Nalge Nunc International, Naperville, IL, USA) (10^5 cells/cm^2, 300 μL media/well) and incubated overnight at 37 °C and 5% CO_2. Cells were rinsed twice and pre-incubated at 37 °C for 1 h in serum-free medium before a 1 to 6 h-incubation in the presence of FGC nanoparticles

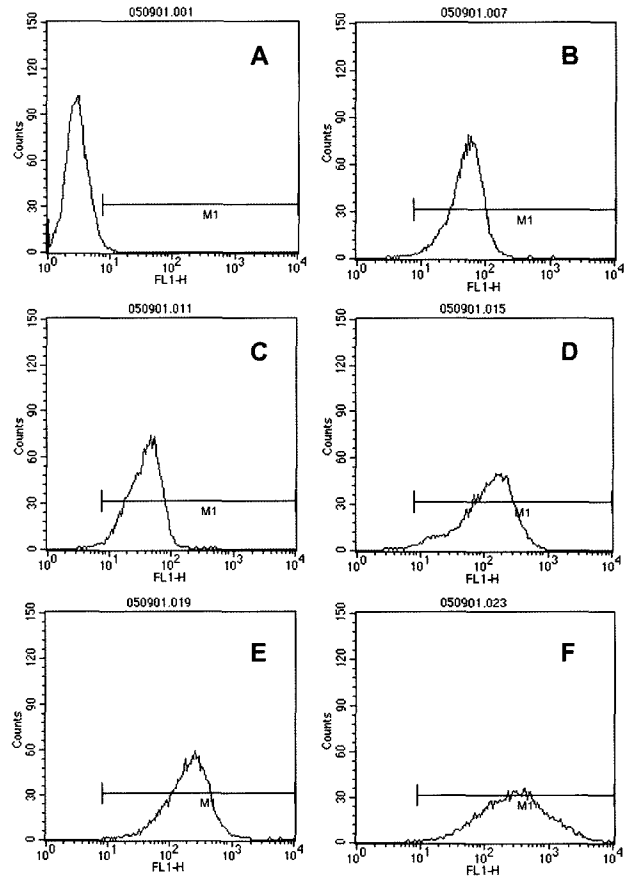

Figure 1. Time-dependent, intracellular uptake of FGC nanoparticles. NIH3T3 cells were incubated in the presence of FGC nanoparticles (0.1 mg/mL) over various incubation times. Control (A), 30 min (B), 1 h (C), 3 h (D), 6 h (E), and 24 h (F) incubation times are shown. After repeated washings to remove free nanoparticles, cells were analyzed by flow cytometry to quantify cellular uptake.

(final particle concentration, 0.2 mg/mL) at 37 °C. The free nanoparticles were aspirated and the cells were then washed three times with PBS (pH 7.4) containing 0.1% BSA. Next, the cells were fixed in a 3.7% paraformaldehyde solution at 4 °C for 15 min. The samples were mounted in fluorescent mounting medium (Dako, Glostrup, Denmark). Images were acquired using a confocal microscope (Nikon Eclipse TE 2000, Tokyo, Japan).

Cell Cycle Analysis by Flow Cytometry. Cells were plated in a 6-well culture dish and cultured at 37 °C in 5% CO_2 until 80% confluent. Next, the cells were rinsed twice, pre-incubated with 2 mL of serum-free medium for 1 h at 37 °C, and then treated with PTX-loaded FGC nanoparticles at 37 °C for periods ranging from 30 min to 24 h. After treatment, the cells were washed three times with 1 mL of PBS (pH 7.4), harvested by trypsinization, washed once with PBS, and fixed in ice-cold 70% ethanol. After fixation, the cells were washed with PBS to remove residual ethanol, pelleted, and re-suspended in propidium iodide (PI) staining buffer (50 μg/mL DNase-free RNase A and 50 μg/mL PI in PBS) for 30 min. Finally, the samples were analyzed using a FACSCalibur flow cytometer.

Results and Discussion

FGC self-assembled nanoparticles were prepared according to the previously reported method.[10,14,15] The isothiocyanate group of FITC reacted easily with the primary amine group of GC. The FITC content as measured by a fluorometer was 2.5 wt%, while the mean diameter as measured by dynamic light scattering was 300 nm. FGC self-assembled nanoparticles had a relatively wide size distribution (polydispersity factor 0.35-0.45).

Cellular Uptake of Nanoparticles. The first barrier to cellular internalization of nanoparticles is the cellular membrane. Chitosan nanoparticles are thought to enter cells via an endocytotic pathway, through either specific (e.g., receptor-mediated endocytosis) or non-specific interactions (e.g., adsorptive endocytosis) with cell membranes.[16,18-20] Uptake of FGC nanoparticles into mouse fibroblast NIH3T3 cells was initiated rapidly within 30 min, as determined by flow cytometry (Figure 1). Even in the absence of ligand binding to specific cell membrane receptors, rapid adsorptive endocytosis of the nanoparticles into NIH3T3 cells seemed to occur. This fast initial uptake of FGC nanoparticles may

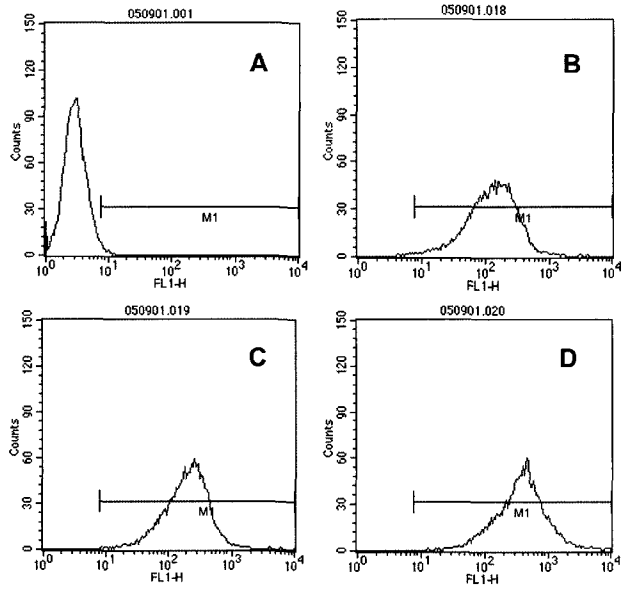

Figure 2. Concentration-dependent, intracellular uptake of FGC nanoparticles. NIH3T3 cells were incubated in the presence of FGC nanoparticles at different concentrations for 6 h. Control (A), 0.05 mg/mL (B), 0.10 mg/mL (C), and 0.50 mg/mL (D) FGC concentrations are shown. After repeated washings to remove free nanoparticles, cells were analyzed by flow cytometry to quantify cellular uptake.

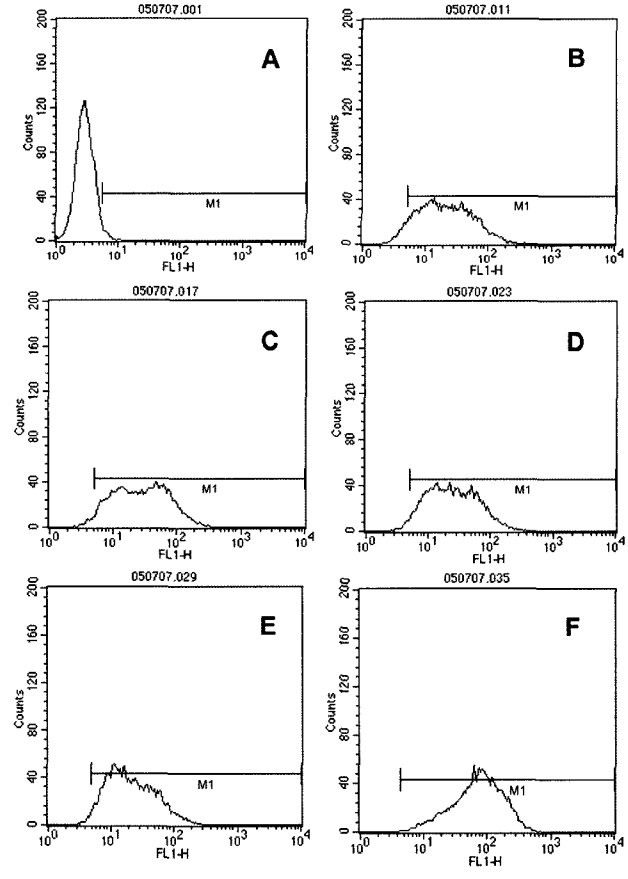

Figure 3. Time-dependent, intracellular uptake of FGC nanoparticles. SCC7 cells were incubated in the presence of FGC nanoparticles (0.10 mg/mL) for different incubation times. Control (A), 30 min (B), 1 h (C), 2 h (D), 4 h (E), and 6 h (F) incubation times are shown. After repeated washing to remove free nanoparticles, cells were analyzed by flow cytometry to quantify cellular uptake.

be attributed to nonspecific electrostatic interactions between the positive zeta potential of chitosan and the possible expression of negative zeta potential on cell membranes. The uptake was saturated within 24 h. Figure 2 shows the concentration-dependent uptake of FGC nanoparticles into NIH3T3 cells. The cellular uptake of FGC nanoparticles increased linearly with FGC concentrations and did not show saturation in the experimental range from 0.05 to 0.50 mg/mL. The NIH3T3 cell viability, as determined by MTT assay, was not affected by FGC nanoparticles in the experimental range from 0.05 to 0.50 mg/mL (data not shown).

Endocytosis and Exocytosis of Nanoparticles. Nanoparticle uptake into mouse squamous carcinoma cells (SCC7) was also initiated rapidly, as shown in Figure 3(B). SCC7 cellular uptake of FGC nanoparticles was dependent upon the incubation time. However, the rate of uptake did not increase linearly with incubation times up to 6 h. A comparison of Figure 3(D) with 3(E) clearly shows that exocytosis should occur as well as endocytosis.

To investigate the dynamics of endocytosis and exocytosis, HeLa cells were incubated with FGC nanoparticles for periods that ranged from 30 min to 6 h, the free nanoparticles were removed, and the cells were incubated in fresh medium for an additional 30 min. When the pre-incubation times were relatively short, such as 30 min (Figures 4(A) and 4(B)) and 1 h (Figures 4(C) and 4(D)), many of the nanoparticles were exocytosed after removing the nanoparticles from the external media. For pre-incubation periods up to 6 h, the amount of exocytosed nanoparticles decreased as the pre-incubation time increased (Figure 4), indicating that exocytosis is dependent on the progress of endocytosis. However, even after a long pre-incubation time (6 h), many nanoparticles were still exocytosed (Figures 4(G) and 4(H)). These results imply that exocytosis could be another important barrier for effective drug delivery into cells using polymer nanoparticles.

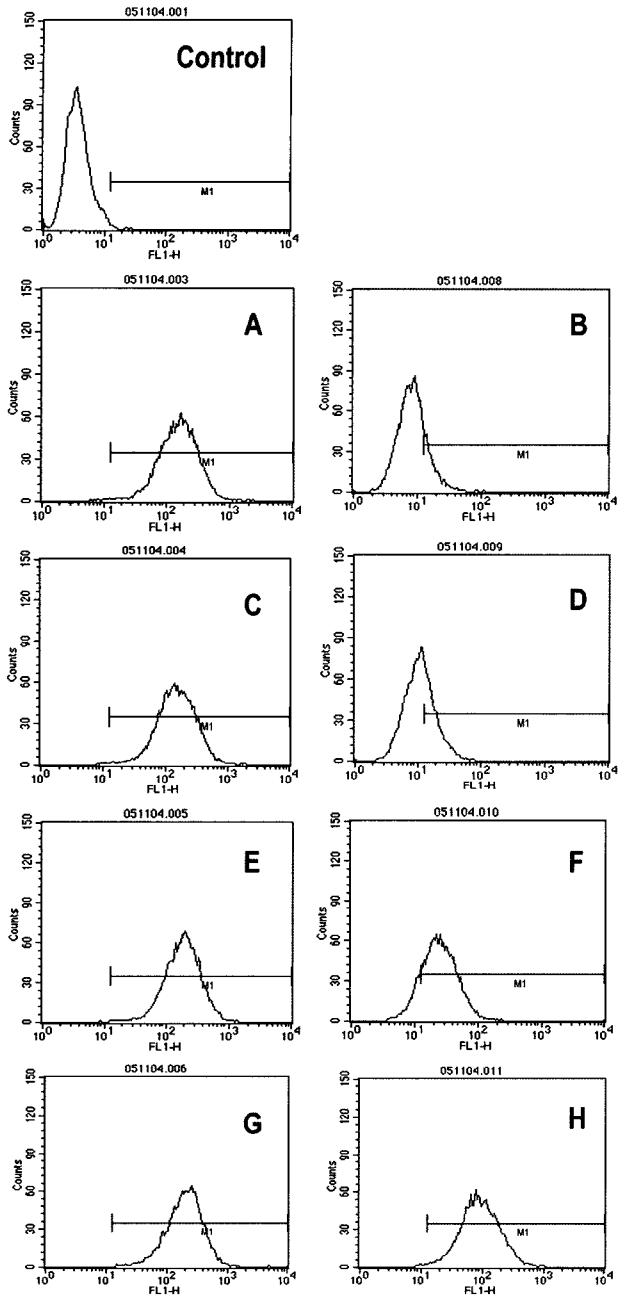

Figure 4. Endocytosis/exocytosis of FGC nanoparticles. HeLa cells were incubated in the presence of FGC nanoparticles (0.05 mg/mL) for 30 min (A, B), 1 h (C, D), 3 h (E, F), and 6 h (G, H). After incubation, free nanoparticles were removed by repeated washing and the cells were incubated in fresh medium for an additional 30 min (B, D, F, and H).

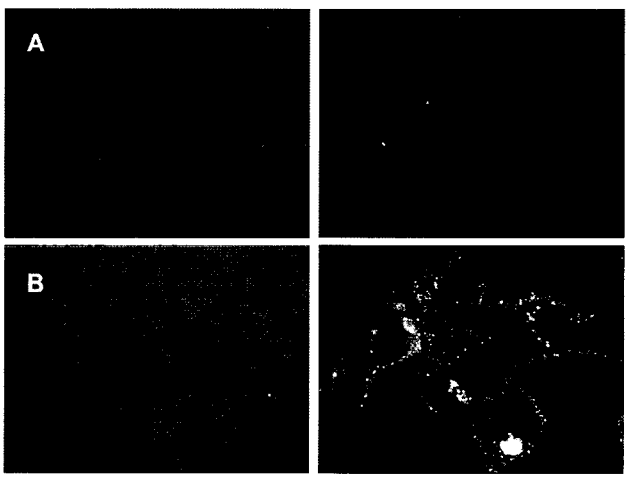

Figure 5. Confocal images of HeLa cells. Cells were incubated in the presence of FGC nanoparticles (0.2 mg/mL) for 1 h (A) and 6 h (B). Green fluorescence indicates the presence of FGC nanoparticles (excitation 490 nm, emission 520 nm). Confocal images of the inner sections of the cells were acquired with constant microscope settings.

Confocal Microscopy. To investigate the internalization and intracellular distribution of FGC nanoparticles, confocal microscopy was performed as shown in Figure 5. Confocal imaging confirmed the cellular internalization of FGC nanoparticles. When HeLa cells were incubated in the presence of FGC nanoparticles (0.2 mg/mL) for 1 h, only weak green fluorescence was observed in the cell membranes and was barely detected inside the cells. However, after 6 h, we clearly observed a strong green fluorescence in the cytoplasm that was indicative of the presence of FGC nanoparticles. The FGC nanoparticles were distributed throughout the cytoplasm as well as in the cell membranes, but no fluorescence was detected in the nuclear compartment.

Effect of FGC Nanoparticles on Cell Cycle Arrest. PTX was incorporated into FGC nanoparticles by the emulsion/solvent evaporation method.[15,20] At a PTX to FGC

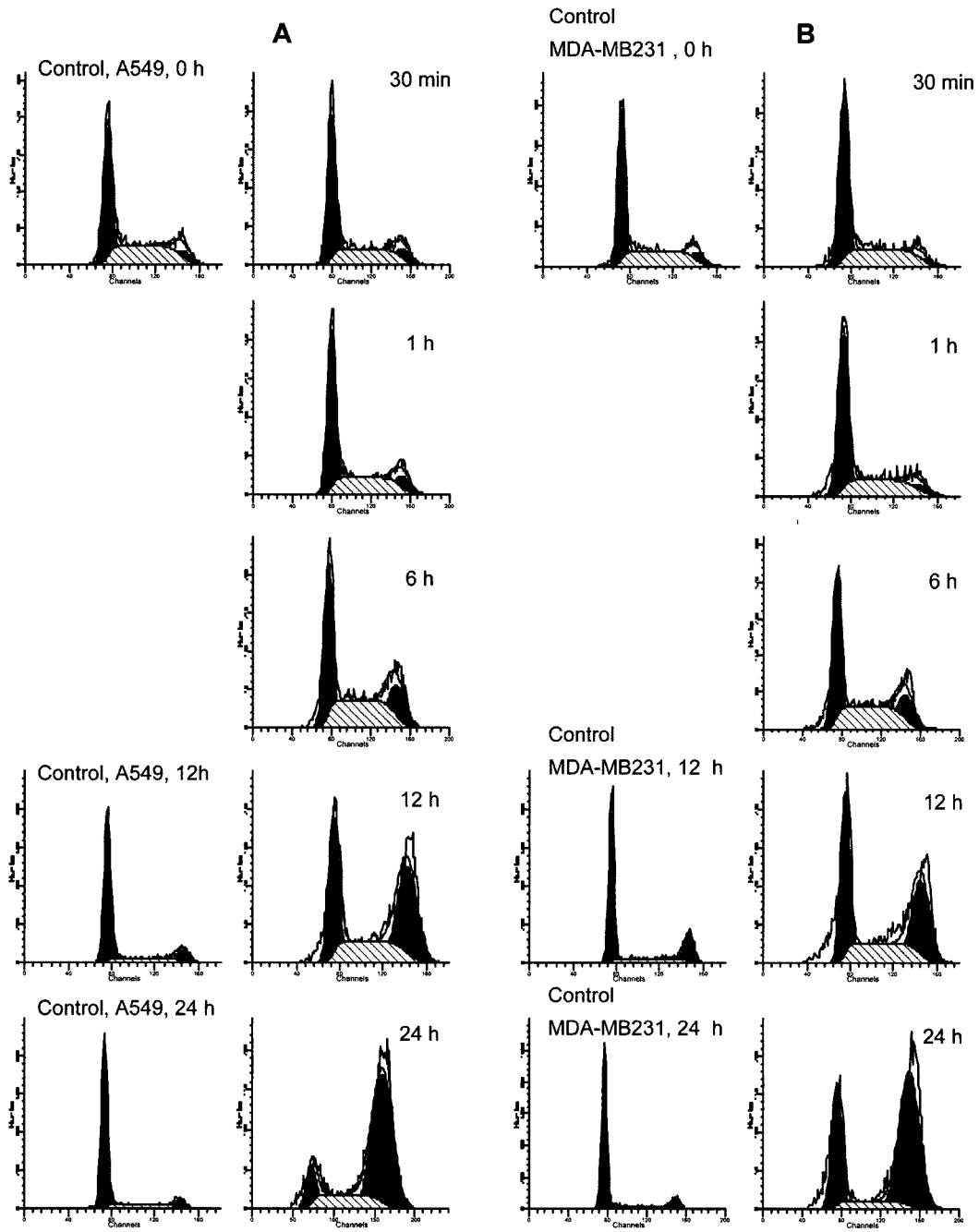

Figure 6. Cell cycle distribution of A549 (A) and MDA-MB231 (B) cells. Cells were incubated in the presence of PTX-loaded FGC nanoparticles and analyzed by flow cytometry. The equivalent PTX concentration was 0.3 μg/mL.

Table I. Cell Cycle Distribution (10,000 cells/count)

A549					MDA-MB231				
Treatment		Cell Cycle Distribution %			Treatment		Cell Cycle Distribution %		
		G0-G1	S	G2-M			G0-G1	S	G2-M
30 min	Control	46.86	43.14	10.01	30 min	Control	52.29	38.62	9.09
	FGC	51.25	37.23	11.52		FGC	57.93	36.77	5.30
1 h	FGC	51.46	36.63	11.91	1 h	FGC	58.63	33.10	8.27
6 h	FGC	38.22	40.74	21.04	6 h	FGC	41.18	39.61	19.21
12 h	Control	66.98	20.90	12.12	12 h	Control	58.24	22.21	19.56
	FGC	31.47	26.98	41.55		FGC	35.13	29.16	35.71
24 h	Control	74.57	18.64	6.78	24 h	Control	74.65	15.64	9.42
	FGC	11.09	21.26	67.65		FGC	27.61	12.12	60.27

nanoparticle feed weight ratio of 0.01, the loading contents of PTX was 0.62 wt%, representing a loading efficiency of 62%. The uptake of PTX-loaded FGC nanoparticles by A549 and MDA-MB231 cells caused cell cycle arrest in the G2-M phase (Figure 6 and Table I). In A549 and MDA-MB231 cells, the G2-M population gradually increased over a 24 h period, from 10% to 67% in the A549 cells and from 9% to 60% in the MDA-MB231 cells. These results indicate the effectiveness of PTX-loaded FGC nanoparticles in the *in vitro* cytotoxicity tests of human cancer cell lines. However, the *in vitro* cytotoxicity results cannot guarantee that PTX-loaded FGC nanoparticles will effectively produce *in vivo* an anti-tumor activity. As mentioned previously, the exocytosis of FGC nanoparticles was greater than expected in cancer cell lines. *In vivo*, the nanoparticles are free of the constraints of the cell culture dish, and thus under these conditions the exocytosed nanoparticles could be transferred to other locations in the body.

Conclusions

FGC nanoparticles were internalized into various cell lines through adsorptive endocytosis by nonspecific interactions between glycol chitosan and cell membranes. However, parts of the endocytosed nanoparticles were exocytosed, particularly in the early stages of endocytosis, suggesting that exocytosis of nanoparticles should be one of important barriers for intracellular drug delivery using polymer nanoparticles. The amount of exocytosed nanoparticles was dependent on the pre-incubation time prior to the removal of free nanoparticles from the culture media. An *in vitro* cytotoxicity assay of human cancer cell lines demonstrated that PTX-incorporated FGC nanoparticles were effective in inducing arrest of cancer cell growth.

Acknowledgements. This work was supported by the Korean Research Foundation Grant funded by the Korean Government (MOEHRD, Basic Research Promotion Fund) (KRF-2006-D00075).

References

(1) G. M. Barratt, *Pharm. Sci. Technol. Today*, **3**, 163 (2000).
(2) R. Duncan, *Nature Rev. Drug Discov.*, **2**, 347 (2003).
(3) L. Brannon-Peppas and J. O. Blanchette, *Adv. Drug. Deliv. Rev.*, **56**, 1649 (2004).
(4) S. Son, S. Y. Chae, C. Choi, M.-Y. Kim, V. G. Ngugen, M.-K. Jang, J.-W. Nah, and J. K. Kweon, *Macromol. Res.*, **12**, 573 (2004).
(5) S. A. Agnihotri, N. N. Mallikarjuna, and T. M. Aminabhavi, *J. Control. Release*, **100**, 5 (2004).
(6) G. Borchard, *Adv. Drug Deliv. Rev.*, **52**, 145 (2001).
(7) K. Kim, J.-H. Kim, S. Kim, H. Chung, K. Choi, I. C. Kwon, J. H. Park, Y.-S. Kim, R.-W. Park, I.-S. Kim, and S. Y. Jeong, *Macromol. Res.*, **13**, 167 (2005).
(8) J. Cha, W. B. Lee, C. R. Park, Y. W. Cho, C.-H. Ahn, and I. C. Kwon, *Macromol. Res.*, **14**, 573 (2006).
(9) K. Y. Lee, W. H. Jo, I. C. Kwon, Y.-H. Kim, and S. Y. Jeong, *Langmuir*, **14**, 2329 (1998).
(10) Y. J. Son, J.-S. Jang, Y. W. Cho, H. Chung, R.-W. Park, I. C. Kwon, I.-S. Kim, J.-Y. Park, S. B. Seo, C. R. Park, and S. Y. Jeong, *J. Control. Release*, **91**, 135 (2003).
(11) J. H. Park, S. Kwon, J.-O. Nam, R.-W. Park, H. Chung, S. B. Seo, I.-S. Kim, I. C. Kwon, and S. Y. Jeong, *J. Control. Release*, **95**, 579 (2004).
(12) J. H. Park, S. Kwon, M. Lee, H. Chung, J. H. Kim, Y. S. Kim, R. W. Park, I. S. Kim, S. B. Seo, I. C. Kwon, and S. Y. Jeong, *Biomaterials*, **27**, 119 (2006).
(13) J. H. Park, Y. W. Cho, Y. J. Son, K. Kim, H. Chung, S. Y. Jeong, K. Choi, C. R. Park, R.-W. Park, I.-S. Kim, and I. C. Kwon, *Colloid Polym. Sci.*, **284**, 763 (2006).
(14) Y. W. Cho, S. A. Park, T. H. Han, D. H. Son, J. S. Park, S. J. Oh, D. H. Moon, K.-J. Cho, C.-H. Ahn, Y. Byun, I.-S. Kim, I. C. Kwon, and S. Y. Kim, *Biomaterials*, **28**, 1236 (2007).
(15) M. Lee, Y. W. Cho, J. H. Park, H. Chung, S. Y. Jeong, K. Choi, D. H. Moon, S. Y. Kim, I.-S. Kim, and I. C. Kwon, *Coll. Polym. Sci.*, **284**, 506 (2006).
(16) M. Huang, E. Khor, and L.-Y. Lim, *Pharm. Res.*, **21**, 344

(2004).
(17) S. M. Moghimi, A. C. Hunter, and J. C. Murray, *Pharmacol. Rev.*, **53**, 283 (2001).
(18) M. Huang, Z. S. Ma, E. Khor, and L.-Y. Lim, *Pham. Res.*, **19**, 1488 (2002).
(19) Z. S. Ma and L.-Y. Lim, *Pharm. Res.*, **20**, 1812 (2003).
(20) J. S. Park, T. H. Han, K. Y. Lee, S. S. Han, J. J. Hwang, D. H. Moon, S. Y. Kim, and Y. W. Cho, *J. Control. Release*, **115**, 37 (2006).